International Electronic Journal of Medicine

Int Electron J Med. 2020; 9(3):124-129

doi 10.34172/iejm.2020.23

Original Article

Evaluation of Lomustine-Loaded Iron Nanoparticles on Caspase-6 Gene Expression and Cell Viability in U87Mg Cell Line

Zeinolabedin Sharifian Dastjerdi[1,2], Elias Kargar Abargouei[1,2], Salman Jafari[3], Ebrahim Eftekhar[2], Majid Pourentezari[4], Fahimeh Zamani Rarani[5], Reza Afzalipour[2,6], Javad Mohajer Ansari[1], Mohammad Zamani Rarani[1,2*]

[1]Department of Anatomical Sciences, Medical School, Hormozgan University of Medical Sciences, Hormozgan, Iran.
[2]Molecular Medicine Research Center, Hormozgan Health Institute, Hormozgan University of Medical Sciences, Bandar Abbas, Iran.
[3]Department of Radiology Technology, School of Paramedicine, Hamadan University of Medical Sciences, Hamadan, Iran.
[4]Department of Biology and Anatomical Sciences, Medical School, Shahid Sadoughi University of Medical Sciences, Yazd, Iran.
[5]Department of Anatomical Sciences, School of Medicine, Isfahan University of Medical Sciences, Isfahan, Iran.
[6]Department of Radiology, Faculty of Para-Medicine, Hormozgan University of Medical Sciences, Bandar Abbas, Iran.

Abstract

Background: Every year, many people around the world die from cancers. Among all types of cancers, brain cancer has been recognized as one of the most deadly cancers due to the late detection and limitations of current therapies, and thus it remains an unresolved problem. Glioblastoma occurs in different parts of the central nervous system and is one of the most important causes of cancer death in people. In addition, there are many problems for the treatment of cancer cells. One of the limiting factors is the resistance of cancer cells to chemotherapy drugs. In this regard, the use of nanoparticles (NPs) is an effective method for overcoming this problem.

Materials and Methods: In this study, iron oxide-NPs were synthesized and loaded on the folic and lomustine. Further, the size and morphology of NPs were assessed by transmission electron microscopy, X-ray photoelectron spectroscopy, and dynamic light scattering. Then, the U87-MG cell line was cultured in the Dulbecco's Modified Eagle Medium and treated with nano, nano-folic, nano-lomustine (LUM), LUM, and complex, followed by evaluating 50% inhibitory concentration, tetrazolium assay, and caspase-6 activity.

Results: Our results showed that cell viability decreased in LUM container groups by increasing the incubation time. Based on the caspase-6 activity analysis, the mortality rate increased in LUM container groups after 3 days. These findings indicated that LUM, complex, and nano-LUM increase cell death in U87MG.

Conclusion: Finally, the results suggested that LUM in NPs could be applied as a safer form of drug delivery for targeting cancer.

Keywords: Targeted therapy, Nanoparticle, Apoptosis, Caspase, U87MG

***Correspondence to**
Mohammad Zamani Rarani, Department of Anatomical Sciences, Medical School, Hormozgan University of Medical Sciences, Hormozgan, Iran.
Molecular Medicine Research Center, Hormozgan Health Institute, Hormozgan University of Medical Sciences, Bandar Abbas, Iran.
Email: mz123esf@gmail.com

Received: April 27, 2020, Accepted: September 12, 2020, ePublished: September 30, 2020

Introduction

Cancer is recognized as one principal cause of mortality worldwide. A large number of people around the world die from cancers every year. In 2012, about 8.2 million deaths from cancer were reported in the world (1). cancer is considered as the third cause of death after cardiovascular diseases and accidents in Iran (2). Among all types of cancers, brain cancer has been identified as one of the most deadly malignancies due to the late detection and limitations of current therapies (3, 4). Researchers have shown that approximately 60% of these tumors are of glioblastoma type (5). Glioblastoma occurs in different parts of the central nervous system and is considered as the main leading cause of cancer death in people under 35 years of age (6, 7). Currently, standard treatments for this type of cancer include surgery and radiation therapy plus chemotherapy (8). After the surgery, the patient undergoes chemotherapy to cure residual cells and metastases (9).

Although this may increase the survival of patients after surgery, the prognosis of this cancer is still not convincing. One of the limiting factors is the resistance of cancer cells to chemotherapy drugs and the low doses of these drugs next to cancerous cells because of the side effects, early renal and liver excretion, as well as the presence of a blood-brain barrier (10, 11). Accordingly, these limiting factors should be eliminated to achieve the desired result. Various methods have been proposed in this regard. The use of nanoparticles (NPs) is an effective and attractive method that has received special attention due to its non-toxicity, the presence of a modifiable surface for coating with biocompatible materials and targeting materials, and the ability to bind to therapeutic molecules (12, 13). NPs can play an important role in the treatment of brain cancer and increase the life span of patients because of the portability of chemotherapeutic drugs, increased drug concentration at the tumor site, and improved drug uptake by cancer cells (14). Chemotherapy drugs can be loaded onto iron oxide (Fe_3O_4) NPs in various ways. The best method is to use polymers with good biocompatibility and biodegradability properties (15). Targeted molecules can also be attached to this polymer and can enhance the specificity and uptake of the complex of nano plus chemotherapeutic drugs. Folic acid (FA) is one of the molecules that is used for targeting therapy with the NP, and its receptors are expressed on many malignant cells, including brain cancer cells (16). In addition, lomustine (LUM) is one of the powerful chemotherapy drugs that can be used to treat these cells. Further, it is a lipophilic drug that has the ability to cross the blood-brain barrier although side effects and therapeutic benefits are not satisfactory. The targeted NPs can increase the uptake of this drug into brain cancer cells and decrease the side effect (17).

Given the above-mentioned explanations, the present study evaluated and compared the effect of nano, nano-folic, nano-LUM, LUM, and complex on cell viability and apoptosis in U87MG brain tumor cells.

Materials and Methods

Nanoparticle Synthesis and Modifications

Fe_3O_4-NPs were synthesized through the standard method. For surface modification, in a bottom of round flask equipped with a condenser and a stirrer, a mixture of APTES (5 mL, Sigma, 440140) and Fe_3O_4 (4.03 g) was refluxed in a dry toluene (100 mL, Sigma, 244511) for 24 hours at 70°C. To separate NPs from the reaction mixture, an external permanent magnet was used, washed with milli-Q water (Sigma) and ethanol for several times, and then dried at 60°C under the vacuum. Next, cyanuric chloride (0.25 g, Sigma, C95501) was added to the mixture (0.50 g) in the dry tetrahydrofuran (40 mL, Sigma, 401756), subsequently, the mixture was stirred for 2 hours at 0°C. The triazine functionalized MNPs (CC-Fe3-O4) were separated from the NP mixture by the magnetic field. Finally, the NPs were washed with tetrahydrofuran several times and dried at 40°C under the vacuum.

Characterization

The size and shape of NPs were determined by TEM (Philips CM10 HT-100 kV). In addition, photoelectron spectroscopy with the X-ray was applied to assess the composition of synthesized NPs. Further, dynamic light scattering was used for sizing NPs and analyzing the hydrodynamic diameter of IONPs (typically ranging between 30 and 190 nm) through the Stokes-Einstein equation. Additionally, IONPs were electrostatically characterized by using the potential (Zeta potential) measurement to determine their surface charge. In general, surface charge, and in turn, the Zeta potential can be modified by employing a polymer coating. Furthermore, 30 mg of nano-LUM was dissolved in phosphate-buffered saline with a pH of 7.4 and digested with ethanol (95% v/v) in order to determine the encapsulation efficiency (EE). After centrifuging at 19400 ×g for 30 minutes, the supernatant was used for analysis. The total mass of LUM in NPs divided by the mass of LUM used in the formulation was considered as EE.

Cell Culture and Group Treatment

The U87-MG cell line was obtained from the Animal Cell Culture Division of Pasteur Institute (Iran, Tehran). The cells were then cultured in DMEM/F12 (Dulbecco's Modified Eagle Medium, Bioidea, Iran) with a 10% FBS (fetal bovine serum, Gibco, Germany), 100 µg/mL of streptomycin (Bioidea, Iran), and 100 U/mL of penicillin (Bioidea, Iran), and kept in a humidified atmosphere at 37°C with 5% CO_2. Nano, nano-folic, nano-LUM, LUM, and complex (nano-folic-LUM) were dissolved in dimethyl sulfoxide (DMSO, Sigma, USA). After the U87-MG cells were more than 80% confluent and growing exponentially, they were counted and plated in a T75 culture flask and incubated with certain concentrations of nano, nano-flic, nano-LUM, LUM, and complex according to the 50% inhibitory concentration (IC50) and the tests were performed at certain times (i.e., 1, 3, and 5 days).

IC50 Assay

This evaluation in U87-MG cells was acquired after 1 day of treatment. Briefly, 10^4 cells were placed into a 12-well plate and treated for 24 hours with various drug concentrations (i.e., 4.25, 7.5, 24.37, and 41.25 µg/mL), and then 3(4, 5-dimethylthiazol-2-yl) 2,5-diphenyl-tetrazolium bromide (MTT, Sigma, the USA) survival assay was carried out to evaluate the cell viability in each group. Next, a percentage of cell viability versus drug concentration was used to obtain the IC50 value.

MTT assay

The effect of control, nano, nano-follicle, nano-LUM,

LUM, and complex on cell viability was determined by the MTT assay. To this end, the U87-MG cell line was cultured in 96-well plates at a density of 10×10^3 cell/well in a culture medium containing 10% FBS and incubated overnight. To evaluate the effect of drugs on cell growth, the cells were treated according to the IC50 value for 1, 3, and 5 day(s). After certain times of incubation in each group, 50 µL of 1 mg/mL MTT tetrazolium salt (Sigma) was added to each well and then the cells were re-incubated at 37°C for 4 hours. Next, the culture medium containing MTT was removed and replaced with 100 µL DMSO (Sigma) to dissolve the produced cell membrane and formazan crystals in lively cells for 2 hours. Finally, absorbance values were read at 570 nm and the percentage of cell viability was estimated using the following formula: Mean optical density (OD) of the treated group/mean OD of the non-treated group ×100

Real-Time Polymerase Chain Reaction for Caspase-6 Expression

U87-MG cells were plated at a density of 5×10^5 in the T27 culture flask overnight and incubated with control, nano, nano-folic, nano-LUM, LUM, and complex for 1, 3, and 7 days according to the IC50 value. After treatment time, the RT-PCR was carried out to determine the caspase-6 expression rate in each group vs. the control group.

Statistical Analysis

One-way analysis of variance with the post-hoc Tukey's test was performed to determine statistical significance among different groups using SPSS software. All quantitative data were presented as the mean ± standard deviation, and acceptable significances were at a level of $P \leq 0.05$.

Results

Nanoparticle Analysis

Figure 1 displays the transmission electron microscopy analysis of LUM-loaded NPs and LUM-loaded NPs modified with FA. It mainly proves that NPs had a spherical shape, and zeta potential values were in the delicate range of -52.4±0.06 to -22.85±0.47 mV. In addition, the poly-dispersity index (particle size distributions), EE, and drug loading content are listed in Table 1. Dynamic light scattering results showed that all synthesized NPs had a hydrodynamic dimension of 19-52 nm. Further, the average size of the hydrodynamic particle was 19.3±0.72, 28.52±0.46, 46.24±1.01, and 52.61±1.12 for magnetic triblock copolymers, magnetic triblock copolymers modified with FA, LUM-loaded magnetic triblock copolymers, and LUM-loaded magnetic triblock copolymers modified with FA, respectively.

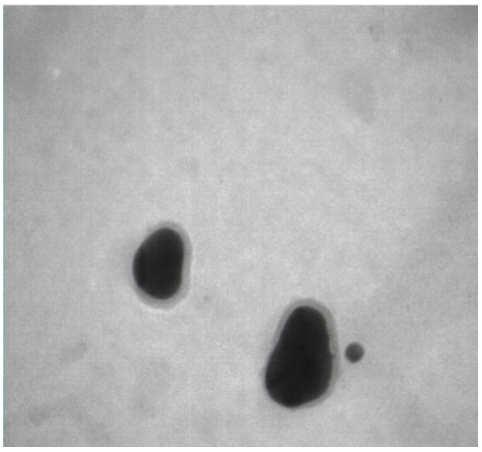

Figure 1. TEM Image of Alginate-IONPs.
Note. TEM: Transmission electron microscopy; IONPs: Iron oxide nanoparticles

Cytotoxicity Assays

The viability of U87Mg cells was determined by the MTT assay for nano, nano-folic, nano-LUM, LUM, and complex drugs. In nano-LUM, LUM, and complex groups, the cell viability decreased by increasing the incubation time (Figure 3).

IC50 Results

The IC50 value was determined by different concentrations of LUM (i.e., 5, 10, 25, 50, 75, 100, 125, & 150 µM). The data results showed that the identified IC50 value (115 µM) by the percentage of inhibition was plotted on nonlinear regression from logarithmic concentrations (Figure 4).

Caspase-6 Expression After the Treatment of the U87-MG Cell Line

Caspase-6 expression analysis was used as an executive apoptotic gene to study the gene expression modified effects of each material in U87MG cell lines. As shown in Figure 5, U87Mg cell treatment with LUM significantly increased in the caspase-6 expression after 3 and 5 days. In nano-LUM and complex, the caspase-6 expression increased compared to the control group as well. However, caspase-6 expression decreased on the fifth day compared to the third day.

Discussion

Attention has focused on the cytotoxicity of NPs by the

Table 1. Properties of NPs (n=3, mean± SD)

NPs	Particle Size (nm)	ζ Potential (mV)	DL%	PDI	EE%
SPION-PEG (NPs)	19.3± 0.72	-52.4±0.06	-	0.11	-
NPs-FA	28.52±0.46	-24.15±0.17	-	0.22	-
LUM-NPs	46.24±1.01	-27.61±0.8	7.34	0.194	68
LUM-NPs-FA	52.61±1.12	-22.85±0.47	6.85	0.25	61

Note. NPs: Nanoparticles; SD: Standard deviation; DL: Drug loading; PDI: Poly-dispersity index; EE: Encapsulation efficiency; SPION-PEG: Superparamagnetic iron oxide nanoparticle-*polyethylene glycol*; FA: Folic acid; LUM: Lomustine.

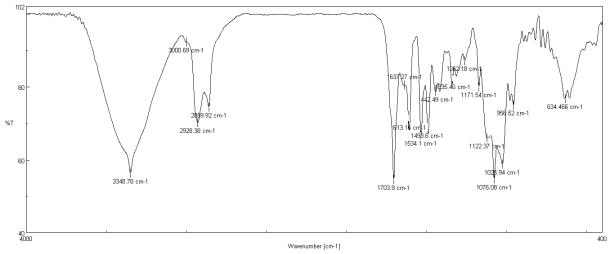

Figure 2. FTIR Spectrum for Lomustine Loaded Nanoparticles.
Note. FTIR: Fourier-transform infrared spectroscopy.

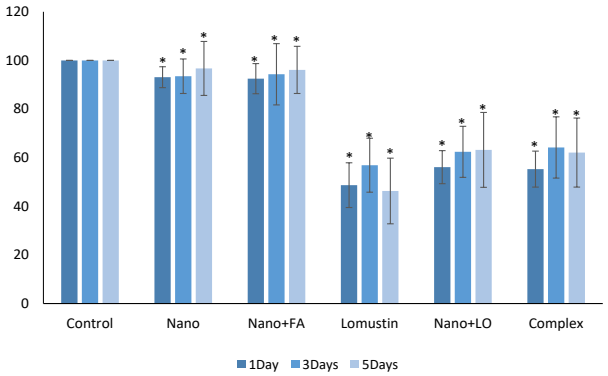

Figure 3. The Effect of Nanoparticles in Cell Viability.

development of nanotechnology applications in medicine (18, 19). NPs are attractive for utilization in various biological fields and have shown commitment to deliver biologic agents to cells (20). Nevertheless, researches demonstrated that NPs have meaningful unacceptable effects on normal cells (21). The characteristics of NPs induce cytotoxicity in cells (22). The manipulation of NPs by biocompatible polymers is required to support the safe utilization in medicine fields (23, 24). Consequently, in our investigation, new modified NP surface by LUM and FA was applied to make a proper nano-size vehicle for medical aims. The results of our study showed that synthesized NPs had a proper size and shape with a super-paramagnetic function. The findings of another study represented that covering the surface of NPs with other drugs makes a decrease in magnetization NPs (25). Therefore, the coating of NPs with drugs can reduce drug concentration (26). Our results are in line with those of Martin et al synthesizing superparamagnetic iron oxide NPs (27).

NP concentrations are important for cytotoxic effects. Based on the results of the present study, NP concentration up to 150 µg/mL had no significant cytotoxic effect after 5 days although the toxic effect increased in higher concentrations, which is compatible with some of the early reports. For example, Yuan et al (28) showed that the viabilities of Hela and C6 cancerous cells represented no reduction with the raised concentration of polyethylene glycol (PEG)- Fe_3O_4 NPs (to 1 mg/mL during 12 hours). Lately, Thapa et al have confirmed that PEG-superparamagnetic iron oxide NPs in the 0.1-10 Mm concentration have no toxic effects on human cancer cells. In another study, NPs influenced the cell apoptosis rate through the stimulation of reactive oxygen species production and then DNA damage, and finally, P53 and caspase-6 overexpression (29). NPs in the cells degenerated into free mineral ions by lysosomal hydrolyzing enzymes (30). Cell organelle such as nucleus or mitochondria can be discharged from free iron ions. In addition, the hydroxyl free radicals effectively react with the DNA chain and some important proteins result in DNA breaks and protein damages and the stimulation of cell apoptosis and death (31). The present study explored the effects of both NPs and LUM-NPs on cell apoptosis and the findings showed that LUM-NPs significantly induced apoptosis in cancerous cells after 3 days.

The caspase-6 activity as apoptosis markers was analyzed to confirm the inhibitory effect of LUM-NP –induced apoptosis. Our results demonstrated that LUM-NPs significantly increased the expression of caspase-6 activity. Other studies also confirmed that caspase has a key role in apoptosis (32, 33). The results of this study further approved that caspase-6 was stimulated by LUM-NPs following 3 days whereas folic NPs and LUM-folic-NPs

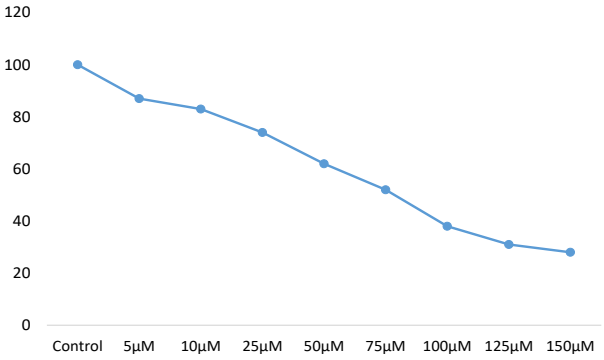

Figure 4. The IC50 Value Determined by Different Concentrations of LUM.

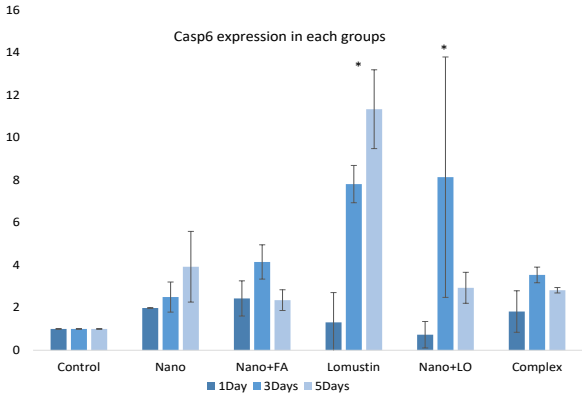

Figure 5. The Effect of Nanoparticles on Caspase-6 Activity in U87-MG Cell Lines.

represented no significant effects on caspase-6 activity. Finally, our results revealed that LUM-NPs induce apoptosis in U87-MG cell lines while NPs and LUM-folic-NPs had no effects on cell programmed death.

Conclusion

In general, our results demonstrated that NPs increased the cytotoxic effects after 5 days when compared with the control group although it was not significant.

Conflict of Interest Disclosures

The authors declared no conflict of interests related to this article.

Acknowledgments

We would like to thank all those who helped us during this project, especially Hormozgan University of Medical Sciences.

Ethical Statement

This study was approved by the Ethics Committee of Hormozgan University of Medical Sciences (IR.HUMS.REC.1396.014).

Authors Contributions

ZSD, EKA, and SJ helped in conducting the study, as well as collecting, analyzing, and interpreting data. In addition, EE, MP, and FZR were responsible for study design, data analysis, and manuscript preparation. Eventually, RA, JMA, MZR, and EKA contributed to conception and design, data collection, analysis, and interpretation, and manuscript writing.

Funding/Support

This study was financially supported by Hormozgan University of Medical Sciences.

Informed Consent

Informed consent was obtained from all individual participants who attended the study.

References

1. Bray F, Ferlay J, Soerjomataram I, Siegel RL, Torre LA, Jemal A. Global cancer statistics 2018: GLOBOCAN estimates of incidence and mortality worldwide for 36 cancers in 185 countries. CA Cancer J Clin. 2018;68(6):394-424. doi: 10.3322/caac.21492.
2. Saadat S, Yousefifard M, Asady H, Moghadas Jafari A, Fayaz M, Hosseini M. The most important causes of death in Iranian population; a retrospective cohort study. Emerg (Tehran). 2015;3(1):16-21.
3. Koo YE, Reddy GR, Bhojani M, Schneider R, Philbert MA, Rehemtulla A, et al. Brain cancer diagnosis and therapy with nanoplatforms. Adv Drug Deliv Rev. 2006;58(14):1556-77. doi: 10.1016/j.addr.2006.09.012.
4. Huse JT, Holland EC. Targeting brain cancer: advances in the molecular pathology of malignant glioma and medulloblastoma. Nat Rev Cancer. 2010;10(5):319-31. doi: 10.1038/nrc2818.
5. Saadatpour L, Fadaee E, Fadaei S, Nassiri Mansour R, Mohammadi M, Mousavi SM, et al. Glioblastoma: exosome and microRNA as novel diagnosis biomarkers. Cancer Gene Ther. 2016;23(12):415-8. doi: 10.1038/cgt.2016.48.
6. Urbańska K, Sokołowska J, Szmidt M, Sysa P. Glioblastoma multiforme - an overview. Contemp Oncol (Pozn). 2014;18(5):307-12. doi: 10.5114/wo.2014.40559.
7. Kelly JJ, Stechishin O, Chojnacki A, Lun X, Sun B, Senger DL, et al. Proliferation of human glioblastoma stem cells occurs independently of exogenous mitogens. Stem Cells. 2009;27(8):1722-33. doi: 10.1002/stem.98.
8. Johnson DR, O'Neill BP. Glioblastoma survival in the United States before and during the temozolomide era. J Neurooncol. 2012;107(2):359-64. doi: 10.1007/s11060-011-0749-4.
9. Pierga JY, Bidard FC, Mathiot C, Brain E, Delaloge S, Giachetti S, et al. Circulating tumor cell detection predicts early metastatic relapse after neoadjuvant chemotherapy in large operable and locally advanced breast cancer in a phase II randomized trial. Clin Cancer Res. 2008;14(21):7004-10. doi: 10.1158/1078-0432.ccr-08-0030.
10. Ozben T. Mechanisms and strategies to overcome multiple drug resistance in cancer. FEBS Lett. 2006;580(12):2903-9. doi: 10.1016/j.febslet.2006.02.020.
11. Florea AM, Büsselberg D. Cisplatin as an anti-tumor drug: cellular mechanisms of activity, drug resistance and induced side effects. Cancers (Basel). 2011;3(1):1351-71. doi: 10.3390/cancers3011351.
12. Mendes M, Sousa JJ, Pais A, Vitorino C. Targeted theranostic nanoparticles for brain tumor treatment. Pharmaceutics. 2018;10(4). doi: 10.3390/pharmaceutics10040181.
13. Agrawal P, Singh RP, Sonali, Kumari L, Sharma G, Koch B, et al. TPGS-chitosan cross-linked targeted nanoparticles for effective brain cancer therapy. Mater Sci Eng C Mater Biol Appl. 2017;74:167-76. doi: 10.1016/j.msec.2017.02.008.
14. Saenz del Burgo L, Hernández RM, Orive G, Pedraz JL. Nanotherapeutic approaches for brain cancer management. Nanomedicine. 2014;10(5):905-19. doi: 10.1016/j.nano.2013.10.001.
15. Vangijzegem T, Stanicki D, Laurent S. Magnetic iron oxide nanoparticles for drug delivery: applications and characteristics. Expert Opin Drug Deliv. 2019;16(1):69-78. doi: 10.1080/17425247.2019.1554647.
16. Boca-Farcau S, Potara M, Simon T, Juhem A, Baldeck P, Astilean S. Folic acid-conjugated, SERS-labeled silver nanotriangles for multimodal detection and targeted photothermal treatment on human ovarian cancer cells. Mol Pharm. 2014;11(2):391-9. doi: 10.1021/mp400300m.
17. Gao H, Yang Z, Zhang S, Cao S, Shen S, Pang Z, et al. Ligand modified nanoparticles increases cell uptake, alters endocytosis and elevates glioma distribution and internalization. Sci Rep. 2013;3:2534. doi: 10.1038/srep02534.
18. Sanna V, Pala N, Sechi M. Targeted therapy using nanotechnology: focus on cancer. Int J Nanomedicine. 2014;9:467-83. doi: 10.2147/ijn.s36654.
19. De Jong WH, Borm PJ. Drug delivery and nanoparticles: applications and hazards. Int J Nanomedicine. 2008;3(2):133-49. doi: 10.2147/ijn.s596.
20. Kulkarni N, Muddapur U. Biosynthesis of metal nanoparticles: a review. J Nanotechnol. 2014;2014:510246. doi: 10.1155/2014/510246.
21. Ahmadian E, Maleki Dizaj S, Rahimpour E, Hasanzadeh A, Eftekhari A, Hosain Zadegan H, et al. Effect of silver nanoparticles in the induction of apoptosis on human hepatocellular carcinoma (HepG2) cell line. Mater Sci Eng C Mater Biol Appl. 2018;93:465-71. doi: 10.1016/j.msec.2018.08.027.
22. Yang X, Liu J, He H, Zhou L, Gong C, Wang X, et al. SiO2 nanoparticles induce cytotoxicity and protein expression alteration in HaCaT cells. Part Fibre Toxicol. 2010;7:1. doi: 10.1186/1743-8977-7-1.
23. Dulińska-Litewka J, Łazarczyk A, Hałubiec P, Szafrański O, Karnas K, Karewicz A. Superparamagnetic iron oxide nanoparticles-current and prospective medical applications. Materials (Basel). 2019;12(4). doi: 10.3390/ma12040617.
24. Han J, Zhao D, Li D, Wang X, Jin Z, Zhao K. Polymer-based

nanomaterials and applications for vaccines and drugs. Polymers (Basel). 2018;10(1). doi: 10.3390/polym10010031.
25. Kliava J, Berger R. Size and shape distribution of magnetic nanoparticles in disordered systems: computer simulations of superparamagnetic resonance spectra. J Magn Magn Mater. 1999;205(2-3):328-42. doi: 10.1016/S0304-8853(99)00510-7.
26. Wang H, Zhao P, Su W, Wang S, Liao Z, Niu R, et al. PLGA/polymeric liposome for targeted drug and gene co-delivery. Biomaterials. 2010;31(33):8741-8. doi: 10.1016/j.biomaterials.2010.07.082.
27. Marinin A. Synthesis and characterization of superparamagnetic iron oxide nanoparticles coated with silica. Digitala Vetenskapliga Arkivet; 2012.
28. Yuan G, Yuan Y, Xu K, Luo Q. Biocompatible PEGylated Fe_3O_4 nanoparticles as photothermal agents for near-infrared light modulated cancer therapy. Int J Mol Sci. 2014;15(10):18776-88. doi: 10.3390/ijms151018776.
29. Wang L, Guo D, Wang Z, Yin X, Wei H, Hu W, et al. Zinc oxide nanoparticles induce human tenon fibroblast apoptosis through reactive oxygen species and caspase signaling pathway. Arch Biochem Biophys. 2020;683:108324. doi: 10.1016/j.abb.2020.108324.
30. Pujalté I, Passagne I, Brouillaud B, Tréguer M, Durand E, Ohayon-Courtès C, et al. Cytotoxicity and oxidative stress induced by different metallic nanoparticles on human kidney cells. Part Fibre Toxicol. 2011;8:10. doi: 10.1186/1743-8977-8-10.
31. Halliwell B, Gutteridge JM. Free Radicals in Biology and Medicine. USA: Oxford University Press; 2015.
32. Saito M, Yaguchi T, Yasuda Y, Nakano T, Nishizaki T. Adenosine suppresses CW2 human colonic cancer growth by inducing apoptosis via A(1) adenosine receptors. Cancer Lett. 2010;290(2):211-5. doi: 10.1016/j.canlet.2009.09.011.
33. Shieh DE, Chen YY, Yen MH, Chiang LC, Lin CC. Emodin-induced apoptosis through p53-dependent pathway in human hepatoma cells. Life Sci. 2004;74(18):2279-90. doi: 10.1016/j.lfs.2003.09.060.